

## CRITICAL SURFACE CONING DUE TO A LINE SINK IN A VERTICAL DRAIN CONTAINING A POROUS MEDIUM

S. AL-ALI<sup>1,2</sup>, G. C. HOCKING<sup>1</sup> and D. E. FARROW<sup>1</sup>

(Received 29 July, 2018; accepted 1 May, 2019; first published online 19 July 2019)

### Abstract

The withdrawal of water with a free surface through a line sink from a two-dimensional, vertical sand column is considered using the hodograph method and a novel spectral method. Hodograph solutions are presented for slow flow and for critical, limiting steady flows, and these are compared with spectral solutions to the steady problem. The spectral method is then extended to obtain unsteady solutions and hence the evolution of the phreatic surface to the steady solutions when they exist. It is found that for each height of the interface there is a unique critical coning value of flow rate, but also that the value obtained is dependent on the flow history.

2010 *Mathematics subject classification*: 0102.

*Keywords and phrases*: coning, line sink, porous media, free surface.

### 1. Introduction

The problem of withdrawal of fluid from a porous medium has many applications in reservoir engineering and aquifer sustainability. The extraction from layers of fluid of different density or other property is of particular interest. The layers may be water of different density or oil and water or natural gas. Previous work shows that fluid from the layer in which the extraction point is placed will alone flow out so long as the flow rate is beneath some critical value [2, 3, 7, 8, 16]. This process is very similar to the problem of stratified withdrawal in surface water [9, 10, 20, 21].

For flow into a line sink in a domain that is unbounded horizontally, a phreatic surface (interface) will not level off at a finite value of height due to the logarithmic nature of the potential function and the surface boundary conditions that must be imposed. McCarthy [15] computed solutions for a line sink in an unbounded horizontal duct by applying pressure conditions at a finite horizontal distance from the inlet. Zhang et al. [11, 25] considered this problem in a vertically confined

<sup>1</sup>Mathematics and Statistics, Murdoch University, Perth, WA, Australia;

e-mail: 32543382@student.murdoch.edu.au, g.hocking@murdoch.edu.au, d.farrow@murdoch.edu.au.

<sup>2</sup>Mathematics Department, College of Sciences and Mathematics, Tikrit University, Saladin, Iraq.

© Australian Mathematical Society 2019

two-dimensional aquifer and used hodograph and numerical methods to find limiting solutions as the flow rate was increased where the interface attached to the horizontal, impermeable boundary at some distance from the sink. Flows in which the limiting steady flow rates were exceeded were computed by Yu [22] and also by Zhang et al. [12, 26] and in three dimensions by Hocking and Zhang [13], and in these papers there were two flowing layers of different density entering the sink. These solutions approached the limiting single layer steady state as the flow rate decreased, although there was some “noise” in the computations that did not allow an accurate determination of the critical values. McCue and Forbes [6] studied a closely related problem with two-dimensional flow due to a line source and a line sink in a horizontally confined region to analyse the optimization of the mineral leaching process.

Here, we investigate the simplified problem of two-dimensional flow into a line sink in a vertical sand column of infinite depth but finite width. The two-dimensional, unsteady problem was considered by Zaradny and Feddes [23] using finite-element methods. Although there are many simplifications in this problem, it is a nice model problem on which to perform some analysis of the physical processes.

The spectral method has recently been used with great success in dealing with surface water hydrodynamics [14, 17] and has been employed to show some interesting effects in plumes and interfaces. One of the purposes of the current work is to determine the efficacy of using similar methods on groundwater flow problems. For that reason, we have chosen a very simple geometry that will enable the computation of some exact solutions for comparison with the method. The hodograph method can be used to find “sub-critical” solutions [4, 18, 19] and also “critical” solutions that appear to be the limiting possible steady flow in any given situation. These are used to verify the spectral method, and then this technique is modified to consider unsteady flows that reveal how the free surface approaches the steady state and what happens at flow rates that exceed the maximum steady flow rate.

## 2. Formulation of the problem

We consider flow of water in a homogeneous, saturated, porous medium in a two-dimensional, vertical column that is confined horizontally with width  $W = 2L$ , with  $-L \leq x \leq L$ , that has an air–water interface (phreatic surface) at the top and is unconfined below, as shown in Figure 1. Water is withdrawn through a line sink of strength (total flux)  $m_0$  located at the origin. The flow will be assumed initially to be steady, with water flowing upward from deep in the column to replenish that removed through the sink. The problem could also be thought of as an infinite set of drains separated by equal distances  $2L$ , as considered by Childs [4], and with a capillary fringe by Youngs [19]. In such a medium, the flow is described by Darcy’s law [1, 5],

$$\mathbf{q} = -\frac{\kappa}{\mu} \nabla \phi, \quad (2.1)$$

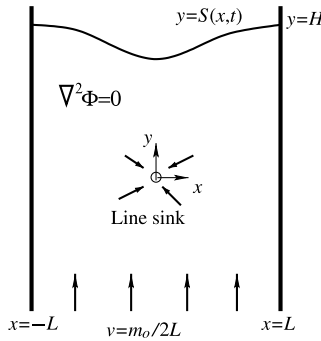


FIGURE 1. Sketch defining the problem variables. The width is  $W = 2L$  and the outer edge of the phreatic surface has elevation  $y = H$ . Total flux into the sink is  $m_0$ , so the upward velocity from deep in the aquifer is  $v = m_0/(2L)$ .

where  $\mathbf{q}$  is the fluid velocity,  $\kappa$  is permeability,  $\mu$  is viscosity, and  $\phi$  is the piezometric head, defined as

$$\phi = \frac{p}{\rho g} + y. \tag{2.2}$$

Here  $\rho$  is the fluid density,  $g$  is gravity,  $p$  is pressure and  $y$  is vertical elevation. In addition, assuming incompressible flow, an equation for conservation of mass is given by

$$\nabla \cdot \mathbf{q} = 0. \tag{2.3}$$

Combining equations (2.1) and (2.3) leads to Laplace’s equation for  $\phi$ , that is,

$$\nabla^2 \phi = 0, \quad -L < x < L, \quad y < S(x, t), \quad t > 0,$$

where  $y = S(x, t)$  is the equation of the (unknown) surface of the saturated zone. There is a line sink at the origin  $(0, 0)$ , so that the piezometric head behaves as

$$\phi \rightarrow \frac{m_0}{2\pi} \log(x^2 + y^2)^{1/2} \quad \text{as } (x, y) \rightarrow (0, 0)$$

where  $m_0$  is the strength of the sink.

There can be no flow through the impermeable boundaries at  $x = \pm L$ , and, invoking the left–right symmetry of the flow, we can write

$$\phi_x(0, y, t) = \phi_x(L, y, t) = 0 \quad \text{on } y < S(x, t), \quad t > 0,$$

and only consider the region  $0 < x < L$ . Now, since the pressure on the free boundary is constant, (2.2) can be written as

$$\phi(x, S(x, t)) = S(x, t) \quad \text{on } y = S(x, t), \quad t > 0.$$

Finally, water particles on the free surface must remain on the surface, leading to the kinematic condition

$$S_t + uS_x - v = 0, \quad \text{on } y = S(x, t), \quad t > 0, \quad 0 < x < L,$$

which in terms of  $\phi$  becomes

$$S_t - \frac{\kappa}{\mu} \phi_x S_x + \frac{\kappa}{\mu} \phi_y = 0 \quad \text{on } y = S(x, t), \quad t > 0, \quad 0 < x < L.$$

Nondimensionalizing with respect to the width  $L$  and the volume flux  $m_0$ , we find the equation becomes

$$\nabla^2 \phi = 0 \tag{2.4}$$

with boundary conditions

$$\phi_x = 0 \quad \text{on } x = 0, \quad x = 1, \quad y < \eta(x, t), \tag{2.5}$$

$$\phi = \eta \quad \text{on } y = \eta(x, t), \quad 0 < x < 1, \tag{2.6}$$

$$\eta_t - \phi_x \eta_x + \phi_y = 0 \quad \text{on } y = \eta(x, t), \quad 0 < x < 1, \tag{2.7}$$

and initial conditions

$$\phi(x, \eta, 0) = \eta(x, 0) = H \quad \text{at } t = 0, \tag{2.8}$$

where  $\eta(x, t)$  is the nondimensional height of the free surface,  $y = H$  is its initial elevation, and all variables are now written in nondimensional form. As the sink is approached, the potential function,  $\phi$  behaves as

$$\phi \rightarrow \frac{m}{2\pi} \log(x^2 + y^2)^{1/2} \quad \text{as } (x, y) \rightarrow (0, 0), \tag{2.9}$$

where  $m$  is a nondimensional sink strength parameter,

$$m = \frac{\mu m_0}{\kappa L}.$$

Since the nondimensional width of the drain is 2 units and the total flux into the sink is  $m$ , the upward velocity from deep in the aquifer must be  $v = m/2$ . The problem is, therefore, to solve the system given by equations (2.4)–(2.8), subject to (2.9).

### 3. Hodograph solutions

The hodograph method [1, 2] can be used to obtain analytical solutions in porous media flows involving a free surface. In this problem, there are two different types of solutions that we may consider, one in which there is a steady-state solution with a stagnation point above the sink and another in which the free surface forms a cusp shape above the line sink. The cusped solution is unique in that it occurs at a single value of flow rate,  $m$ , for a given geometrical configuration and is thought to represent the limiting steady flow before the drawdown of the interface directly into the sink. In the hodograph method, we introduce a mapping noting that for a steady flow  $\eta_t \equiv 0$  and the kinematic condition (2.7) can be combined with the dynamic condition (2.6). Differentiating along the free surface in terms of the arclength  $s$ ,

$$\phi'(s) = \eta'(s),$$

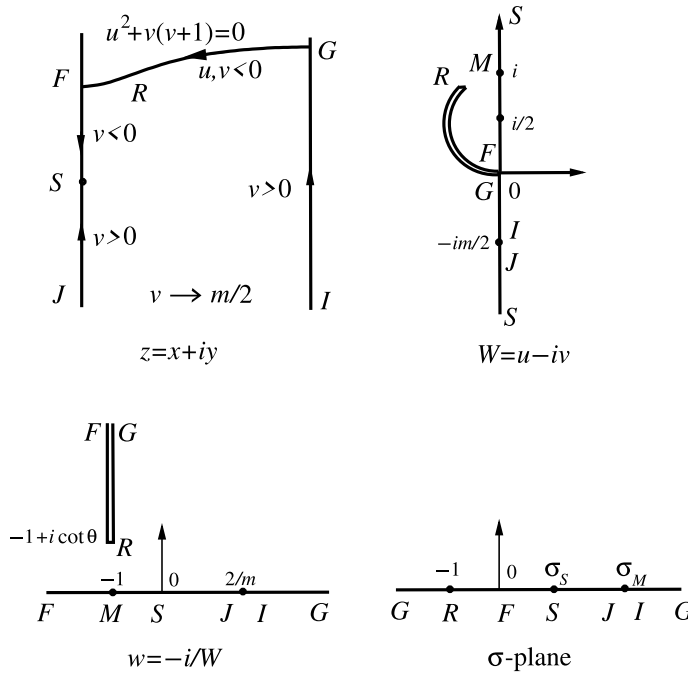


FIGURE 2. Mappings used to obtain the hodograph solution for the sub-critical solution. The physical  $z = (x + iy)$ -plane and the hodograph  $W = u - iv$  are linked via the  $w$ - and  $\sigma$ -planes to find an exact expression for the flow.

where the ' denotes the derivative with respect to the independent variable, we find that

$$\phi_x x'(s) + \phi_y y'(s) = \eta'(x) \frac{dx}{ds} \Rightarrow \phi_x + \phi_y \eta'(x) = \eta'(x)$$

on  $y = \eta(x)$ . Substituting into (2.7) with  $\eta_t \equiv 0$  gives

$$\phi_x^2 + \phi_y(\phi_y - 1) = 0 = u^2 + v(v + 1). \tag{3.1}$$

Therefore, if we define  $f(z) = \phi + i\psi$  to be a function in the complex  $z$ -plane, then the points defined by (3.1) lie on a circle with centre  $(0, 1/2)$ , and radius  $1/2$  in the  $W = (u - iv)$ -plane, as shown in Figures 2 and 3. The function  $\psi(x, y)$  is the equivalent of the streamfunction in surface water flows, and can be used to plot streamlines. The important feature of using this technique is to map the region of interest to a region in which the solution can be written down by inspection. In both sub-critical and critical flow solutions described here, this turns out to be a half-plane containing appropriately placed sources and sinks.

**3.1. Sub-critical flow** The particular solution for sub-critical flow that involves a stagnation point on the surface is given by Childs [4] and Van Deemter [18], but

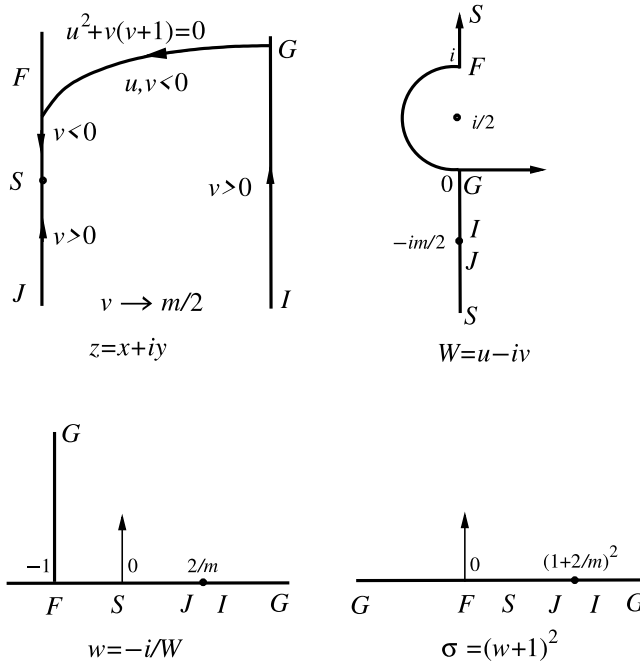


FIGURE 3. Mappings in the hodograph solution for the critical, cusped solution. The planes used are named similarly to those in Figure 2 for consistency and to show the similarities.

we repeat the details here for completeness. The crucial feature of this process is the mapping of the hodograph plane to the half-plane, and the main features are demonstrated in Figure 2.

We note that in the physical  $z = (x + iy)$ -plane we can specify various quantitative features of the velocity. In this case, the speed of flow must be zero at points  $F$  and  $G$ , and it is clear that the horizontal component of velocity is zero on  $F$  to  $S$ ,  $S$  to  $J$  and  $I$  to  $G$  and thus lies on the vertical axis in the  $W = u - iv = -f'(z)$ -plane (see Figure 2). We can also say that the vertical component is positive,  $v > 0$ , on  $I$  to  $G$  and  $J$  to  $S$ , while it must be negative,  $v < 0$ , on  $F$  to  $S$ . The free surface  $FG$  must lie on the circle as described above. The incomplete circle  $GRF$  involves a cut as the air-water interface becomes steeper, reaches a maximum slope of  $v/u$ , and then becomes shallower to reach point  $F$  where the flow is stagnant. The point deep in the duct  $IJ$  has a vertical upward flux of  $m/2$  as the total flux  $m$  is split across a width of 2 from the symmetry of the situation, and so in the hodograph plane this point appears on the vertical axis. Clearly the speed of flow slows on the vertical “wall” at  $x = 1$ , eventually slowing to zero at  $G$ , while it speeds up as the sink is approached from  $J$  to  $S$ , so that the sink itself lies at  $|W| \rightarrow \infty$ .

In order to best write down the solution, it is now necessary to map the hodograph plane to the upper half-plane. In this case this is a mathematical transaction. To begin,

the inversion of  $w = 1/(iW) = 1/(iu + v)$  maps the hodograph to the upper-half of  $w$ -plane, involving a vertical cut  $w = -1 + ir, r \geq \cot \theta$ , as shown, where  $\theta$  is the angle of the steepest point on the phreatic surface. The next step is the mapping

$$w = \frac{1}{2}(\sigma - 1)\sigma^{-1/2} \cot \theta - 1 = iz'(f) \tag{3.2}$$

to map to the half-plane as indicated. In this plane, we can write the potential function

$$f(z) = -\frac{m}{2\pi} [\log(\sigma - \sigma_S) - \log(\sigma - \sigma_M)] \tag{3.3}$$

that consists of a mathematical sink at  $\sigma = \sigma_S$  and a mathematical source at  $\sigma = \sigma_M$ . The source point represents the point,  $IJ$ , deep in the aquifer from which the water is replenished, but appears as a point in the  $\sigma$ -plane. It remains to compute the location of the free surface from these computations, in other words, a bridge between  $z$  and  $f$  via the mappings. One approach to this is to find

$$z'(\sigma) = z'(f)f'(\sigma),$$

the components of which can be determined from (3.2) and (3.3), leading to

$$z'(\sigma) = \frac{mi}{2\pi} \left( \frac{1}{2}(\sigma - 1)\sigma^{-1/2} \cot \theta - 1 \right) \left( \frac{-1}{\sigma - \sigma_S} + \frac{1}{\sigma - \sigma_M} \right),$$

where

$$\sigma_S = \kappa_S + \sqrt{\kappa_S^2 - 1}$$

with  $\kappa_S = 1 + 2 \tan^2 \theta$ , and  $\sigma_M$  satisfies

$$\sigma_M = \kappa_M + \sqrt{\kappa_M^2 - 1}$$

with  $\kappa_M = 1 + 2(1 + 2/m)^2 \tan^2 \theta$ .

This solution needs to be scaled with respect to the width of the drain, to compare with the nondimensional width across the top of the drain, and so we note that the “width” of the drain from the mapped form is

$$X_L = \frac{m}{4} \cot \theta \left( \frac{\sigma_M - 1}{\sqrt{\sigma_M}} - \frac{\sigma_S - 1}{\sqrt{\sigma_S}} \right),$$

and the total deflection of the phreatic surface is

$$Y_L = \frac{m}{2\pi X_L} \log \left( \frac{\sigma_M}{\sigma_S} \right). \tag{3.4}$$

The shape of the phreatic surface can be found from

$$\begin{aligned} x(\sigma) &= \frac{m}{4\pi X_L} \cot \theta \int_0^\sigma \frac{\sigma - 1}{(-\sigma)^{1/2}} \left( \frac{1}{\sigma - \sigma_M} - \frac{1}{\sigma - \sigma_S} \right) d\sigma \\ &= \frac{m}{2\pi X_L} \cot \theta \left[ \left( \frac{\sigma_M - 1}{\sqrt{\sigma_M}} \right) \tan^{-1} \sqrt{\frac{-\sigma}{\sigma_M}} - \left( \frac{\sigma_S - 1}{\sqrt{\sigma_S}} \right) \tan^{-1} \sqrt{\frac{-\sigma}{\sigma_S}} \right], \end{aligned}$$

$$y(\sigma) = -\frac{m}{2\pi X_L} \int_0^\sigma \left( \frac{1}{\sigma - \sigma_M} - \frac{1}{\sigma - \sigma_S} \right) d\sigma$$

$$= -\frac{m}{2\pi X_L} \log \left[ \left( \frac{\sigma_M - \sigma}{\sigma_S - \sigma} \right) \left( \frac{\sigma_S}{\sigma_M} \right) \right],$$

noting that  $-\infty < \sigma < 0$  corresponds to the phreatic surface. In addition, the distance from the sink to the phreatic surface above the sink can be determined to be

$$\Delta y_{SF} = \frac{m}{2\pi} \cot \theta \left( \frac{\sigma_S - 1}{\sqrt{\sigma_S}} \coth^{-1} \sqrt{\sigma_S} - \frac{\sigma_M - 1}{\sqrt{\sigma_M}} \coth^{-1} \sqrt{\sigma_M} \right), \tag{3.5}$$

so that the total distance from the sink to the phreatic surface on the outer edge of the drain (at point  $G$ ) is  $\Delta y_{SG} = \Delta y_{SF} + Y_L$  from (3.5) and (3.4), respectively. These solutions will be presented later in comparison with the steady solution obtained using the spectral method.

**3.2. Critical flow** In the limit as the maximum slope angle approaches  $\theta \rightarrow \pi/2$ , the solution above approaches the critical case in which the solution cones into a vertical cusp. Unfortunately, the limit as  $\theta \rightarrow \pi/2$  in the mapping (3.2) is not simple, and so we describe the modification here that gives the critical flow case.

Observing the velocity along the solid boundaries of the flow domain, we notice that the boundary at  $x = 0$  beneath the sink,  $SJ$ , corresponds to the line  $JS$  in the  $w$ -plane, as  $u = 0$ ,  $m/2 < v < \infty$ , noting that  $v \rightarrow \infty$  as the sink is approached. The boundary at  $GI$  has  $u = 0$  and  $0 < v < m/2$ , so corresponds to  $GI$  in the  $W$ -plane. The line  $x = 0$  above the sink  $SF$  in the  $z$ -plane corresponds to  $SF$  in the  $W$ -plane, where  $-\infty < v < -1$ , and  $v = -1$  corresponds to the cusp point on the free surface. The point  $G$  at  $z = 1 + iH$  also has the property that  $u = v = 0$ , and is a stagnation point, while the point  $IJ$  at  $v = m/2$  corresponds to the point deep in the aquifer from which the water emanates. The mappings required are shown in Figure 3.

As above, we now proceed to map the  $W$ -plane to the upper-half of the  $\sigma$ -plane via an intermediate mapping, so that the solution for the sink flow can be written down. Mapping  $w = -i/W = -iz'(f)$  to the  $w$ -plane as shown in Figure 3, and then the  $w$ -plane to the lower-half of  $\sigma$ -plane with

$$\sigma = (w + 1)^2 \Rightarrow w = -1 + \sigma^{1/2},$$

we can write the solution for the sink flow in the  $\sigma$ -plane. In the  $\sigma$ -plane, the complex potential for flow into the sink can be written as

$$f(\sigma) = \frac{m}{2\pi} (\log(\sigma - 1) - \log(\sigma - \kappa^2)),$$

where  $\kappa = (1 + 2/m)$ , which corresponds to a source at  $\sigma = \kappa^2$  and a sink at  $\sigma = 1$ . As above, this source represents the flow from deep in the aquifer at  $IJ$ . Therefore, we can find

$$z'(\sigma) = z'(f)f'(\sigma) = -\frac{mi}{2\pi} (-1 + \sigma^{1/2}) \left( \frac{1}{\sigma - 1} - \frac{1}{\sigma - \kappa^2} \right).$$

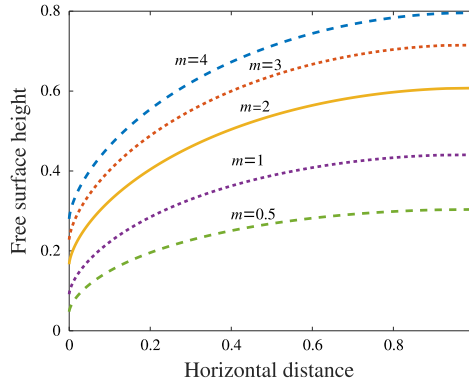


FIGURE 4. Interface shapes for the hodograph critical flow solutions for  $m = 4, 3, 2, 1, 0.5$ . The shape is a typical cusp shape. Higher  $m$  occurs when the surface is at a greater height above the sink, indicating more suction is required.

From this equation we obtain the distance from the sink to the surface,  $SF$ , as

$$\begin{aligned} \Delta y_{SF} &= -\frac{m}{2\pi} \int_0^1 (\sigma^{1/2} - 1) \left( \frac{1}{\sigma - 1} - \frac{1}{\sigma - \kappa^2} \right) d\sigma \\ &= -\frac{m}{2\pi} \left[ \log\left(\frac{\kappa^2 - 1}{4\kappa^2}\right) + 2\kappa \tanh^{-1}(1/\kappa) \right], \end{aligned}$$

and the shape of the phreatic surface can be found from

$$\begin{aligned} x(\sigma) &= \frac{m}{2\pi} \int_0^\sigma (-\sigma)^{1/2} \left( \frac{1}{\sigma - 1} - \frac{1}{\sigma - \kappa^2} \right) d\sigma \\ &= \frac{m}{\pi} \left( \kappa \tan^{-1} \sqrt{\frac{-\sigma}{\kappa^2}} - \tan^{-1} \sqrt{-\sigma} \right), \\ y(\sigma) &= \frac{m}{2\pi} \int_0^\sigma \left( \frac{1}{\sigma - 1} - \frac{1}{\sigma - \kappa^2} \right) d\sigma \\ &= \frac{m}{2\pi} \log\left(\frac{1 - \sigma}{1 - \sigma/\kappa^2}\right), \end{aligned}$$

noting that  $-\infty < \sigma < 0$  corresponds to the surface.

Figure 4 shows several solutions for different values of  $m$ . As the critical height of the interface increases, a larger  $m$  value is required to pull the interface down into the cusp shape.

#### 4. Steady sub-critical solutions

The cusped coning solution is often cited to be the maximum flow at which steady solutions exist [8, 15, 24, 25]. If the flow rate becomes higher then the surface draws down directly into the sink, and if there is a layer of fluid of different density above

then it will begin to flow into the sink [26]. In this section we will use a spectral method to compute flows in which the flow rate is below the critical value. A verification that the maximal flow corresponds to the critical hodograph solutions is obtained if the maximal value of  $m$  for each steady-state solution matches the corresponding critical case.

The method is to find a solution as a combination of a flow in the vertical column plus a spectral component that satisfies all but the surface conditions on  $y = \eta(x)$ .

The steady version of equations (2.4)–(2.8) is

$$\nabla^2 \phi = 0, \tag{4.1}$$

$$\phi_x = 0 \quad \text{on } x = 0, x = 1, y < \eta(x), \tag{4.2}$$

$$\phi = \eta \quad \text{on } y = \eta(x), 0 < x < 1, \tag{4.3}$$

$$\phi_x \eta_x - \phi_y = 0 \quad \text{on } y = \eta(x), 0 < x < 1. \tag{4.4}$$

The two-dimensional column solution will provide the solution for flow with no free surface, but will ensure the satisfaction of all of the conditions except for those on the free surface. We choose to write

$$\phi = \phi_D + \Phi, \tag{4.5}$$

where  $\phi_D$  is the flow from a vertical column into a line sink. Noting that  $\Phi$  is an even function, we choose the form

$$\Phi = a_0 - \frac{m}{4}y + \sum_{k=0}^{\infty} a_k e^{\lambda_k \eta} \cos(\lambda_k x) \quad \text{where } \lambda_k = k\pi. \tag{4.6}$$

The coefficients  $a_k, k = 0, 1, 2, \dots$ , will be determined by the conditions on the flow. The term  $-m/4$  is required to obtain the correct flux into the sink. As  $y \rightarrow -\infty, \phi_D$  approaches  $-m/4$ , and so the combination gives upward flux of  $m/2$ , since the total flux into the centrally located sink is  $m$  over a width of 2 units (by symmetry). Above the height of the sink, this term cancels the downward flux from  $\phi_D$ , in this case  $m/4$ . Thus the flux into the sink is  $m/2$ , with all of the water coming up from below, since there is no recharge at the phreatic surface. Ultimately we will need to determine the coefficients  $a_k = 0, 1, 2, \dots$  that satisfy the free surface conditions. To proceed from here, we must find the solution for flow in a vertical duct.

The complex potential for such a flow is easily shown to be

$$f_D = \frac{m}{2\pi} \log \left[ 2i \sin \left( \frac{\pi z}{2} \right) \right],$$

for which  $\phi_D$ , the real part, is

$$\phi_D = \frac{m}{2\pi} \log \left[ 4 \cosh^2 \left( \frac{\pi y}{2} \right) - 4 \cos^2 \left( \frac{\pi x}{2} \right) \right]^{1/2}.$$

A natural choice for the form of the shape of the free surface is

$$\eta = H + \sum_{k=0}^{\infty} b_k \cos(\lambda_k x) \quad \text{where } \lambda_k = k\pi, \tag{4.7}$$

since this is compatible with the form of  $\phi$ , where the coefficients  $b_k, k = 1, 2, 3, \dots$ , are to be determined.

**4.1. Linear steady solution** The form of  $\phi$  given by (4.5) with (4.6) is such that all conditions (2.5)–(2.7) are satisfied, except those on the unknown surface,  $y = \eta(x)$ . In general, to find the shape of the surface is a nonlinear problem, but if we assume the disturbance of the surface to be relatively small, we can compute a linearized solution by considering the disturbance about the mean height  $y = H$ .

The linearized conditions on  $y = H$  are

$$\eta = \phi \quad \text{on } y = H, \quad 0 < x < 1, \tag{4.8}$$

$$\phi_y = 0 \quad \text{on } y = H, \quad 0 < x < 1. \tag{4.9}$$

Noting that

$$\phi_y = \phi_{D_y} - \frac{m}{4} + \sum_{k=0}^{\infty} a_k \lambda_k e^{\lambda_k H} \cos(\lambda_k x) \quad \text{when } y = H,$$

where

$$\phi_{D_y}(x, y) = -\frac{m}{8} \left( \frac{\sinh(\pi y)}{\cosh^2(\pi y/2) - \cos^2(\pi x/2)} \right),$$

the unknown coefficients  $a_k$ ,  $k = 0, 1, 2, \dots$ , can be found using orthogonality in (4.9), as  $\Phi_y(x, H) = -\phi_{D_y}(x, H)$ , leading to

$$a_k = -\frac{2}{\lambda_k e^{\lambda_k H}} \int_0^1 \phi_{D_y}(x, H) \cos(k\pi x) dx, \quad k = 1, 2, \dots$$

However, it is possible to compute this solution exactly. Using a variation on the mapping  $f_D$  that includes an image sink at  $y = 2H$  gives a complex potential function for the linearized problem,  $f_{LIN}$ , that satisfies (4.9) exactly, namely,

$$f_{LIN} = \frac{m}{2\pi} \log[(1 - e^{-i\pi z})(e^{i\pi z} - e^{-2\pi H})],$$

of which the real part is

$$\phi_{LIN} = \frac{m}{4\pi} \log[((e^{-\pi y} + Ae^{\pi y}) \cos(\pi x) - A - 1)^2 + ((e^{-\pi y} - Ae^{\pi y}) \sin(\pi x))^2],$$

where  $A = \exp(-2\pi H)$ . Then, applying (4.8), the shape of the surface for any  $m$  and  $H$  can be found to be

$$\eta_{LIN} = H + \frac{m}{4\pi} \log \left[ \frac{A + 1 - 2e^{-\pi H} \cos(\pi x)}{2e^{-\pi H} + A + 1} \right].$$

This solution can be compared to the full nonlinear solution.

**4.2. Nonlinear solution** In the full problem, we need to solve the system (4.1)–(4.4). In principle, we can use the same approach, but the orthogonality of the components no longer holds, because all of the calculations must now be performed on  $y = \eta(x)$  rather than on  $y = H$  (as in the linear case).

The equation for  $\eta(x, t)$  (4.7) is equally appropriate here, and substituting for this and  $\phi$  in the pressure condition (4.3), multiplying by  $\cos \lambda_j x$  and integrating from 0 to 1 gives an integral expression for the coefficients,  $b_j, j = 1, 2, \dots$ , as

$$\sum_{k=1}^N b_k \int_0^1 \cos(\lambda_k x) \cos(\lambda_j x) dx + H \int_0^1 \cos(\lambda_j x) dx - \int_0^1 \left( \phi_D + \sum_{k=0}^{\infty} a_k e^{\lambda_k \eta} \cos(\lambda_k x) \right) \cos(\lambda_j x) dx = 0$$

for each  $j = 1, 2, \dots, N$ , after truncating the series to  $N$  terms. Exploiting the orthogonality of the eigenfunctions, we find

$$\left( 1 + \frac{m}{4} \right) H - a_0 - \int_0^1 \left( \phi_D + \sum_{k=0}^{\infty} a_k e^{\lambda_k \eta} \cos(\lambda_k x) \right) dx = 0 \tag{4.10}$$

and

$$\frac{1}{2} \left( 1 + \frac{m}{4} \right) b_j - \int_0^1 \left( \phi_D + \sum_{k=0}^{\infty} a_k e^{\lambda_k \eta} \cos(\lambda_k x) \right) \cos(\lambda_j x) dx = 0, \quad j = 1, 2, \dots, N - 1. \tag{4.11}$$

This provides us with  $N$  equations, but we have  $2N$  unknowns in the  $a_j, b_j$ , and so we can invoke a similar process for the kinematic condition (4.4). Noting that the derivative of (4.7) is

$$\eta'(x) = - \sum_{k=0}^{\infty} b_k \lambda_k \sin(\lambda_k x),$$

and  $\phi_x$  can be found by differentiating the function (4.5) with respect to  $x$ ,

$$\phi_x = \phi_{D_x} - \sum_{k=0}^{\infty} a_k \lambda_k e^{\lambda_k \eta} \sin(\lambda_k x),$$

we can employ these substitutions in (4.4). Applying the operation as above, it follows that

$$\int_0^1 \left( \phi_{D_y} + \sum_{k=0}^{\infty} a_k \lambda_k e^{\lambda_k \eta} \cos(\lambda_k x) \right) \cos(\lambda_j x) dx - \int_0^1 \left( \phi_{D_x} + \sum_{k=0}^{\infty} a_k e^{\lambda_k \eta} \lambda_k \sin(\lambda_k x) \right) \left( \sum_{k=0}^{\infty} b_k \lambda_k \sin(\lambda_k x) \right) \cos(\lambda_j x) dx = 0, \tag{4.12}$$

$j = 1, 2, \dots, N.$

This provides a further  $N$  equations, and so the combination of (4.10), (4.11) and (4.12) gives  $2N$  nonlinear equations for the  $2N$  unknowns.

The function `fsolve` in MATLAB™ was used to solve this nonlinear system of equations. Once the coefficients of the series have been obtained, it is possible to

TABLE 1. Fourier coefficients,  $a_k$ , for the potential function,  $\phi(x)$ , for different values of number of coefficients,  $N$ , for the case of  $m_{\max} = 2.34$  and  $H = 0.84$ . This case is close to the critical case. Coefficients are converged to 4 decimal places by  $N = 30$ , and are effectively zero by  $a_{20}$  for this situation.

$a_k$	Fourier series coefficients, $a_k$					
	$N = 10$	$N = 20$	$N = 30$	$N = 40$	$N = 50$	$N = 100$
$a_1$	-0.0307	-0.0307	-0.0307	-0.0307	-0.0307	-0.0307
$a_2$	-0.0125	-0.0125	-0.0125	-0.0125	-0.0125	-0.0125
$a_3$	-0.006	-0.006	-0.006	-0.006	-0.006	-0.006
$a_4$	-0.0029	-0.0029	-0.0029	-0.0029	-0.0029	-0.0029
$a_5$	-0.0014	-0.0014	-0.0014	-0.0014	-0.0014	-0.0014
$a_6$	-0.0008	-0.0008	-0.0008	-0.0008	-0.0008	-0.0008
$a_7$	-0.0005	-0.0005	-0.0005	-0.0005	-0.0005	-0.0005
$a_8$	-0.0003	-0.0003	-0.0003	-0.0003	-0.0003	-0.0003
$a_9$	-0.0002	-0.0002	-0.0002	-0.0002	-0.0002	-0.0002
$a_{10}$	-0.0002	-0.0002	-0.0002	-0.0002	-0.0002	-0.0002
$a_{20}$		0	0	0	0	0
$a_{30}$			0	0	0	0
$a_{40}$				0	0	0
$a_{50}$					0	0
$a_{100}$						0

compute the numerical values for the shape of the free surface  $\eta(x)$ . Integration was performed using Gaussian quadrature. The convergence of the coefficients in the series is shown in Tables 1 and 2. It is clear that the series have both converged to 4 decimal places by the 30th coefficient, and are zero to 4 decimal places by  $a_k$ ,  $k = 40$ , so that no more than  $N = 50$  is required to obtain converged solutions. Graphically, these sub-critical solutions agree exactly with those of the sub-critical hodograph method.

**4.3. The results** The results of some of the steady solutions are shown in Figure 5, along with their linear counterparts (dashed lines), for the case where the mean surface height is  $H = 0.5$  and  $m = 0.5, 1, 2$ . It is clear that as  $m$  increases the linear solution varies more from the full nonlinear solutions, but this comparison verifies the implementation of the scheme to be correct. For any fixed mean water surface height,  $H$ , there are multiple steady solutions as  $m$  increases, but only up to a maximum value of  $m_{\max}$ . As the height  $H$  decreases, this critical value of  $m_{\max}$  decreases as would be expected since less pressure variation is required to pull down the surface. The largest value of  $m$  ( $m = 2$ ) shown in Figure 5 is not far from the limiting value for existence of the steady state, and it has the characteristic shape of a pre-coning surface. This suggests that there is a maximum flow rate beyond which the surface draws down into the sink.

Figure 6 shows a comparison of the steady surface shape for several values of  $m$  compared with the cusped hodograph solution at the same value of  $H$ . It seems that the

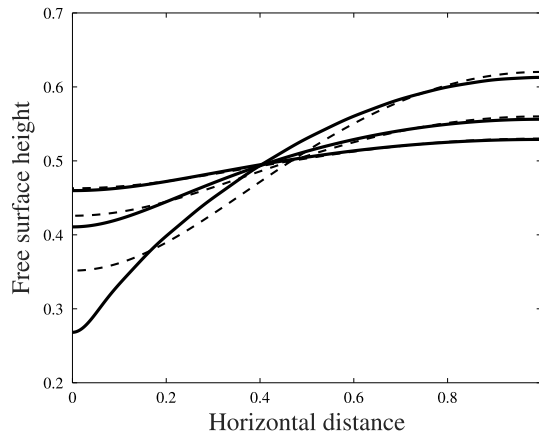


FIGURE 5. Comparison of steady free surface shapes for a mean surface height of  $H = 0.5$  and values of flow  $m = 0.5, 1$  and  $2$ . The dashed lines are the linear solution, the solid the full nonlinear. The case  $m = 2$  is just below the maximal steady state. The sub-critical hodograph solutions agree to graphical accuracy with the spectral solutions.

TABLE 2. Fourier coefficients,  $b_k$ , for the surface shape,  $\eta(x)$ , for different values of number of coefficients,  $N$ , for the case of  $m_{\max} = 2.34$  and  $H = 0.84$ . This case is close to critical. Coefficients are converged to 4 decimal places by  $N = 30$ , and are effectively zero by  $b_{30}$  for this situation.

$b_k$	Fourier series coefficients, $b_k$					
	$N = 10$	$N = 20$	$N = 30$	$N = 40$	$N = 50$	$N = 100$
$b_1$	-0.1672	-0.1677	-0.1677	-0.1677	-0.1677	-0.1677
$b_2$	-0.0438	-0.0442	-0.0442	-0.0442	-0.0442	-0.0442
$b_3$	-0.0166	-0.0169	-0.0169	-0.0169	-0.0169	-0.0169
$b_4$	-0.0084	-0.0087	-0.0087	-0.0087	-0.0087	-0.0087
$b_5$	-0.0053	-0.0056	-0.0056	-0.0056	-0.0056	-0.0056
$b_6$	-0.0036	-0.0038	-0.0039	-0.0039	-0.0039	-0.0039
$b_7$	-0.0024	-0.0027	-0.0027	-0.0027	-0.0027	-0.0027
$b_8$	-0.0016	-0.0019	-0.0019	-0.0019	-0.0019	-0.0019
$b_9$	-0.0011	-0.0014	-0.0014	-0.0014	-0.0014	-0.0014
$b_{10}$	-0.0008	-0.001	-0.0011	-0.0011	-0.0011	-0.0011
$b_{20}$		-0.0001	-0.0001	-0.0001	-0.0001	-0.0001
$b_{30}$			0	0	0	0
$b_{40}$				0	0	0
$b_{50}$					0	0
$b_{100}$						0

surface shapes of the steady solutions approach the shape of the cusped (hodograph) solution as the maximal  $m$  is approached. The sub-critical hodograph solution and the

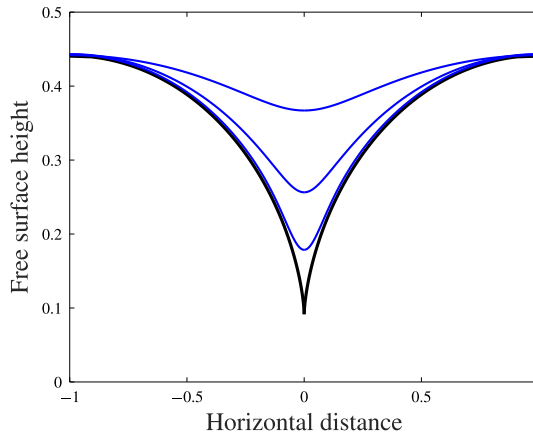


FIGURE 6. Steady, sub-critical interface shapes with an outer height of  $H = 0.44$  and deepening as  $m$  changes from  $m = 0.4, 0.8$  to  $0.95$ , compared with the critical hodograph surface with the cusp shape at  $m = 1$ .

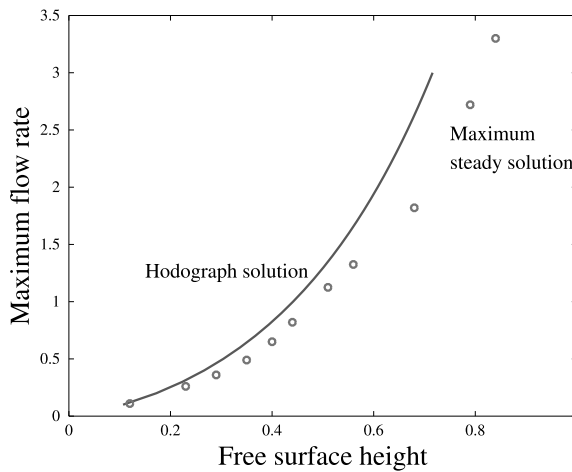


FIGURE 7. Maximum flow rate  $m_{\max}$  obtained using the spectral method for different heights compared with the critical hodograph solution for the same surface heights. The solid line is the critical hodograph solution. It is clear that the maximal steady state agrees very well with the cusped, drawdown solution. The maximal sub-critical hodograph solutions match almost exactly with the critical solution curve.

spectral steady solutions are graphically identical, but the spectral method does not converge for very steep interface shapes as the limit is approached.

The values of the maximum flow rate  $m_{\max}$  for different surface heights compared with the hodograph solution are shown in Figure 7. As  $H$  increases, the value of  $m_{\max}$  for the steady solutions obtained with the spectral method drop a little below the critical hodograph solutions, but in general the steady solutions exist up until the

formation of the cusped solution and not beyond. This result is as expected, but we can consider the behaviour at higher values of flow rate,  $m$ , by examining unsteady flows.

### 5. Unsteady flow

We have obtained solutions to the steady problem using both the hodograph method and the spectral method, and shown that the upper flux limit of these corresponds closely to the cusped hodograph solutions. In order to consider what happens at higher flow values,  $m$ , we can adapt the method to derive an unsteady solution procedure. To do this, we can use the same basic formula as the steady problem but allow the coefficients to become functions of time. Time variation can be determined via equation (2.7). Differentiating the now time-varying version of  $\eta$  gives

$$\eta_t(x, t) = H'(t) + \sum_{k=0}^{\infty} b'_k(t) \cos(\lambda_k x), \quad \lambda_k = k\pi,$$

and, substituting into (2.7) and using orthogonality where appropriate, we find

$$\begin{aligned} H'(t) = & -\frac{m}{4} - \int_0^1 \left( \phi_{D_y} + \sum_{k=0}^{\infty} a_k \lambda_k e^{\lambda_k \eta} \cos(\lambda_k x) \right) dx \\ & + \int_0^1 \left( \phi_{D_x} + \sum_{k=0}^{\infty} a_k e^{\lambda_k \eta} \lambda_k \sin(\lambda_k x) \right) \left( \sum_{k=0}^{\infty} b_k \lambda_k \sin(\lambda_k x) \right) dx \end{aligned} \tag{5.1}$$

and

$$\begin{aligned} \frac{1}{2} b'_j(t) = & - \int_0^1 \left( \phi_{D_y} + \sum_{k=0}^{\infty} a_k \lambda_k e^{\lambda_k \eta} \cos(\lambda_k x) \right) \cos(\lambda_j x) dx \\ & + \int_0^1 \left( \phi_{D_x} + \sum_{k=0}^{\infty} a_k e^{\lambda_k \eta} \lambda_k \sin(\lambda_k x) \right) \left( \sum_{k=0}^{\infty} b_k \lambda_k \sin(\lambda_k x) \right) \cos(\lambda_j x) dx, \\ & j = 1, 2, \dots, N. \end{aligned} \tag{5.2}$$

The values of  $b_j(t)$ ,  $j = 1, 2, \dots, N$  are then updated simultaneously with the dynamic condition in the form of (4.10) and (4.11) to find the new values of  $a_j(t)$ ,  $j = 1, 2, \dots$ , using a fourth-order Runge–Kutta scheme. Again, `fsolve` must be used to find the values of  $a_j(t)$ ,  $j = 1, 2, \dots$ , at each step.

At  $t = 0$ ,  $\eta = H$ , and  $b_j(0) = 0$ ,  $j = 1, 2, \dots, N$ , so invoking orthogonality at this initial time,

$$a_j(0) = -2 \int_0^1 \phi_D(x, H) e^{\lambda_j H} \cos(\lambda_j x) dx$$

are the initial values for  $j = 1, 2, 3, \dots, N$ .  $H(t)$  is again the mean height of the free surface.

**5.1. Linear solution** Just as in the steady situation, we can compute a simplified linear solution by making the calculations at  $y = H(t)$  as time proceeds. This is a reasonable assumption so long as the deflection of the surface is only small. In that case, the linearized equations are

$$\eta_t = -\phi_y(x, H(t)),$$

which leads to

$$H'(t) = -\frac{m}{4} - \int_0^1 \phi_{Dy}(x, H) dx,$$

$$b'_j(t) = -2 \int_0^1 \phi_{Dy}(x, H) \cos(\lambda_j x) dx - a_j \lambda_j e^{\lambda_j H}, \quad j = 1, 2, \dots, N,$$

and also

$$a_0 = \left(1 + \frac{m}{4}\right)H - \int_0^1 \phi_D(x, H) dx,$$

$$a_j = b_j \left(1 + \frac{m}{4}\right) e^{-\lambda_j H} - 2e^{-\lambda_j H} \int_0^1 \phi_D(x, H) \cos(\lambda_j x) dx, \quad j = 1, 2, \dots, N.$$

Thus we can step through time using numerical integration and the results can be compared with the full nonlinear solution. Using this approach, every value of  $H$  has a steady solution for any  $m$  (although some may be unrealistic with the surface located below the sink) and the numerical scheme approaches the linear steady-state solutions as obtained above. An interesting feature of these unsteady, linear solutions is that the mean height of the interface remains constant, so that the surface at the outer edge rises up while the point above the sink is pulled downward. This slightly surprising result suggests that for any situation there are multiple solutions that depend on the location of the interface before the flow begins. It also suggests that the critical condition will depend to some extent on the flow history.

For the full nonlinear problem, solutions will not exist for sufficiently large  $m$ , as the sink draws the phreatic surface downward into the sink. No solutions of the linear equations are shown, but at smaller values of  $m$  and larger  $H$  they follow the nonlinear solutions closely, thus verifying the nonlinear method. However, the drawdown cannot be determined by the linear solutions, and so, just as for the steady case, we must consider the full nonlinear solution.

**5.2. Nonlinear solution** In the nonlinear problem, we have the same steps as for the linear, but the equations must be determined on  $y = \eta(x, t)$  rather than on  $y = H(t)$ . We step through time using a fourth-order Runge–Kutta scheme for equations (5.1), (5.2) and (4.10), (4.11). The values of the coefficients  $a_j$ ,  $j = 1, 2, 3, \dots$ , must be computed iteratively at each sub-step of the Runge–Kutta scheme. At any time, the value of  $H(t)$  is close to the average height of the surface.

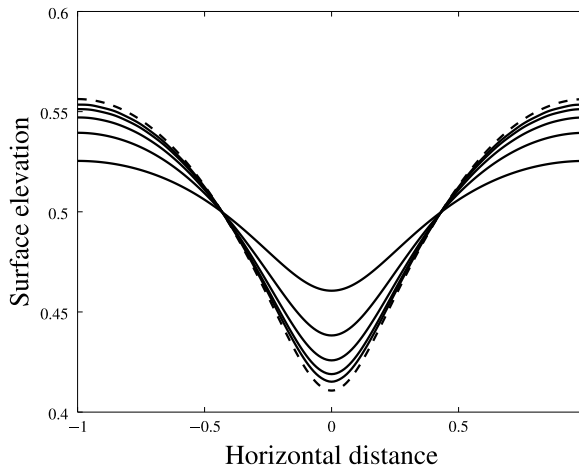


FIGURE 8. Surface shapes at times  $t = 0.2, 0.4, 0.6, 0.8, 1.0$  for  $H = 0.5$ ,  $m = 1.0$ . The dashed line is the steady state solution for this value of  $m$ . The surface is clearly approaching the steady solution as  $t \rightarrow \infty$ . The central dip increases in depth as time increases while the outer edges rise, but movement slows as the steady solution is approached.

In principle, the method can be used to solve for any flow rate and any starting values. The first results sought were those in which the initial height and value of  $m$  were such that the free surface should approach a steady-state solution. Figure 8 shows this convergence for the case  $H = 1$ ,  $m = 1$ , with the dip in the centre growing until it reaches the steady solution. In all cases of sub-critical  $m$  the surface rapidly evolved to the steady-state solution for the corresponding parameter values. Interestingly, for all of these cases the mean height of the surface remained the same and the phreatic surface simply adjusted to satisfy the pressure condition, exactly as in the case of the linear solutions. This is reasonable, as the infinite depth of the column allows the water to flow upward from below the sink to maintain the level. These solutions provide a nice verification of the method.

The real interest here is in what happens if the flow value  $m$  is above the expected steady limit. A series of simulations was performed and it was found that if such a value was chosen, the middle of the free surface continued to travel downward towards the outlet point until the method failed, even as the outer edge rose slightly as in the sub-critical cases. The elevation of the deepest point on the surface for a starting depth of  $H = 0.5$  as a function of time for several different values of flow rate  $m$  is shown in Figure 9. At this value of  $H$  the limiting steady state solution is at  $m = 1.3$ . At smaller values of  $m$  the deepest point levels off, while for values greater than  $m = 1.3$  it continues to travel downward with higher speed. The value at  $m = 1.5$  is only just above the highest steady value, and so appears to level off, but the surface continues to travel downward until the method fails. The curves for  $m = 1.5, 2.0$  and  $2.5$  terminate at the points at which the method fails to converge. The likely reason for the failure is that the middle of the interface moves extremely fast and is essentially singular in time.

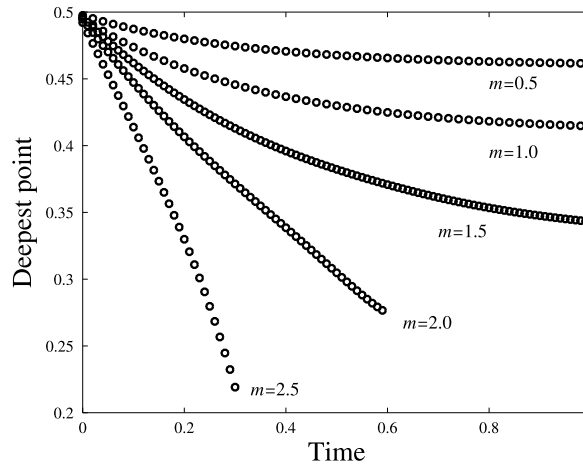


FIGURE 9. The elevation of the deepest point on the surface as a function of time for different values of  $m = 0.5, 1.0, 1.5, 2.0, 2.5$ . The limiting steady solution for this case is when  $m = 1.32$ , between the cases  $m = 1.0$  and  $m = 1.5$ . Values of  $m$  smaller than this level off with time, while those at larger  $m$  continue to travel downward.

It is very difficult to capture this moment in the code without using exceptionally small time steps. The failure is characterized by the formation of oscillations of numerical origin on the interface close to the outer edges.

## 6. Conclusion

The withdrawal of water through a line sink from within a two-dimensional vertical column of infinite depth containing some porous medium is considered. Hodograph solutions are presented for both sub-critical and critical steady solutions, and compared to a spectral method that has been used to solve both the steady and unsteady versions of the problem. The spectral and hodograph solutions are in excellent agreement for sub-critical flow rates. Clearly, this situation is slightly unrealistic, but could be a model for withdrawal near to the interface in a stratified aquifer of great depth. However, more importantly, the model clearly identifies the important factors in the process and the behaviour of the interface as water is withdrawn.

In all unsteady simulations, the mean level of the phreatic surface or interface remains approximately constant, except in cases where a steady solution does not exist. If the flow rate is sufficiently small, the surface simply adjusts to the steady-state solution, while if it is large enough the middle of the surface pulls down in a narrowing cone at an approximately linear rate until it draws into the sink. The existence of steady solutions at many different heights for different values of flow rate strongly suggests that the steady solution that is finally “chosen” depends on the history of the flow. Therefore, in order to determine which steady solution will evolve it is important to know the history. The drawn-down (cusped) solutions, on the

other hand, are unique for each value of  $H$ , as illustrated by the hodograph solution. Therefore, if the starting conditions are such that the interface lies above the line given by the hodograph solutions in Figure 7, that is, the initial  $H$  value is below the value of the critical coning solution, then the outcome will almost certainly be coning, leading to drawdown of the interface.

## References

- [1] J. Bear, *Dynamics of fluids in porous media* (McGraw-Hill, New York, 1972).
- [2] J. Bear and G. Dagan, "Some exact solutions of interface problems by means of the hodograph method", *J. Geophys. Res.* **69** (1964) 1563–1572; doi:10.1029/JZ069i008p01563.
- [3] J. R. Blake and A. Kucera, "Coning in oil reservoirs", *Math. Sci.* **13** (1988) 36–47; [http://www.appliedprobability.org/data/files/TMS%20articles/13\\_1\\_6.pdf](http://www.appliedprobability.org/data/files/TMS%20articles/13_1_6.pdf).
- [4] E. C. Childs, "A treatment of the capillary fringe in the theory of drainage", *J. Soil Sci.* **10** (1959) 83–100; doi:10.1111/j.1365-2389.1959.tb00668.x.
- [5] H. Darcy, *Fontaines publiques de la ville de Dijon* (ed. V. Dalmont), (Librairie des Corps imperiaux des ponts et chaussées et des mines, 1856).
- [6] L. K. Forbes and S. W. McCue, "Optimal fluid injection-strategies for in situ mineral leaching in two-dimensions", *J. Eng. Math.* **36** (1999) 185–206; doi:10.1023/A:1004406311441.
- [7] F. M. Giger, "Analytic 2-D models of water cresting before breakthrough for horizontal wells", *SPE Res. Eng.* **4** (1989) 409–416; doi:10.2118/15378-PA.
- [8] E. J. Hinch, "The recovery of oil from underground reservoirs", *J. Physico-Chem. Hydrodynamics* **6** (1985) 601–622; doi:10.1016/B978-0-444-87707-9.50017-8.
- [9] G. C. Hocking, "Supercritical withdrawal from a two-layer fluid through a line sink", *J. Fluid Mech.* **297** (1995) 37–47; doi:10.1017/S0022112095002990.
- [10] G. C. Hocking and L. K. Forbes, "Supercritical withdrawal from a two-layer fluid through a line sink if the lower layer is of finite depth", *J. Fluid Mech.* **428** (2001) 333–348; doi:10.1017/S0022112000002780.
- [11] G. C. Hocking and H. Zhang, "A note on withdrawal from a two-layer fluid through a line sink in a porous medium", *ANZIAM J.* **50** (2008) 101–110; doi:10.1017/S144618110800028X.
- [12] G. C. Hocking and H. Zhang, "Coning during withdrawal from two fluids of different density in a porous medium", *J. Eng. Math.* **65** (2009) 101–109; doi:10.1007/s10665-009-9267-1.
- [13] G. C. Hocking and H. Zhang, "A note on axisymmetric supercritical coning in a porous medium", *ANZIAM J.* **55** (2014) 327–335; doi:10.1017/S1446181114000170.
- [14] N. A. Letchford, L. K. Forbes and G. C. Hocking, "Inviscid and viscous models of axisymmetric fluid jets or plumes", *ANZIAM J.* **53** (2012) 228–250; doi:10.1017/S1446181112000156.
- [15] J. F. McCarthy, "Gas and water cresting towards horizontal wells", *ANZIAM J.* **35** (1993) 174–197; doi:10.1017/S0334270000009115.
- [16] M. Muskat and R. D. Wyckoff, "An approximate theory of water coning in oil production", *Amer. Inst. Mining Engineers, Petroleum Development Technol.* **114** (1935) 144–163; doi:10.2118/935144-G.
- [17] P. Russell, L. K. Forbes and G. C. Hocking, "The initiation of a planar fluid plume beneath a rigid lid", *J. Eng. Math.* **106** (2017) 107–121; doi:10.1007/s10665-016-9895-1.
- [18] J. J. Van Deemter, "Bijdragen tot de kennis van enige natuurkundige grootheden van de grond" *Versl. Landb. Onderz.* **56** (1950) 1–67.
- [19] E. G. Youngs, "Effect of the capillary fringe on steady-state water tables in drained lands", *J. Irrigation Drainage Eng.* **138** (2012) 803–814; doi:10.1061/(asce)ir.1943-4774.0000467.
- [20] C. S. Yih, *Stratified Flows*, 2nd edn (Academic Press, New York, 1980).
- [21] C. S. Yih, "On steady stratified flows in porous media", *Quart. J. Appl. Math.* **40** (1982) 219–230; doi:10.1090/qam/666676.

- [22] D. Yu, K. Jackson and T. C. Harmon, "Dispersion and diffusion in porous media under supercritical conditions", *Chem. Eng. Sci.* **54** (1999) 357–367; doi:10.1016/S0009-2509(98)00271-1.
- [23] H. Zaradny and R. A. Feddes, "Calculation of non-steady flow towards a drain in saturated-unsaturated soil by finite elements", *Agricultural Water Management* **2** (1979) 37–53; doi:10.1016/0378-3774(79)90012-X.
- [24] H. Zhang and G. C. Hocking, "Axisymmetric flow in an oil reservoir of finite depth caused by a point sink above an oil-water interface", *J. Eng. Math.* **32** (1997) 365–376; doi:10.1023/A:1004227232732.
- [25] H. Zhang, G. C. Hocking and D. A. Barry, "An analytical solution for critical withdrawal of layered fluid through a line sink in a porous medium", *ANZIAM J.* **39** (1997) 271–279; doi:10.1017/S0334270000008845.
- [26] H. Zhang, G. C. Hocking and B. Seymour, "Critical and supercritical withdrawal from a two-layer fluid through a line sink in a partially bounded aquifer", *Adv. Water Res.* **32** (2009) 1703–1710; doi:10.1016/j.advwatres.2009.09.002.